〔千葉医学 77：221～229, 2001〕

〔Original Paper〕

Longitudinal base to apex perfusion gradients by dipyridamole positron emission tomography indicate diffuse coronary atherosclerosis

Yuko Nakagawa

(Received December 19, 2000, Accepted January 16, 2001)

SUMMARY

Diffuse coronary atherosclerosis is clinically important and often associated with localized stenosis but is not detected or quantified by current methods including coronary arteriography. Accordingly, I quantified the longitudinal base to apex distribution of N-13 ammonia on positron emission tomography (PET) after dipyridamole stress for 17 normal volunteers and 30 patients with abnormal coronary arteriograms. Heart images were divided into 32 short axis tomographic slices along the long axis, and each slice was divided into anterior, septal, lateral and inferior quadrant. Average relative activity for each slice in each quadrant was graphed against slice number and a third order polynomial curve was best fit to the longitudinal distribution of activity. In the patients group, average relative activity in each quadrant, except septum in mild to moderate disease group, progressively and significantly decreased from base to apex slices compared to normal group, and perfusion decreasing was more progressed in severe disease group. In 12 of the patients with one- or two-vessel disease, longitudinal base to apex perfusion gradient was observed in angiographically stenosis-free quadrant. Thus, patients with segmental coronary artery disease by arteriography have abnormal longitudinal base to apex perfusion gradients on dipyridamole PET images indicating diffuse coronary atherosclerosis.

Key words: longitudinal perfusion gradient, positron emission tomography, coronary disease, atherosclerosis

I. Introduction

Diffuse coronary atherosclerosis is clinically important[1-3] and is common in association with mild or severe localized stenosis but is not detected or quantified by current non-invasive methods or standard coronary arteriography (CAG)[4]. Fluid dynamic analysis indicates that diffuse coronary atherosclerosis causes a longitudinal base to

3rd Department of Internal Medicine, School of Medicine, Chiba University, Chiba 260-8670.
中川優子：ジピリダモール負荷ポジトロンCTを用いた心基部から心尖部にかけての長軸方向の血流解析による瀰漫性冠動脈硬化の評価.
千葉大学医学部内科学第三講座 Tel. 043-222-7171.
2000年12月19日受付, 2001年1月16日受理.

apex perfusion gradient with highest perfusion at the base decreasing gradually to lowest perfusion at the apex. To evaluate diffuse coronary artery narrowing, I quantified the longitudinal base to apex distribution of N-13 ammonia on positron emission tomography (PET) images after dipyridamole stress in patients with 20% diameter stenosis or greater by coronary arteriography to define one, two and three vessel disease.

II. Materials and Methods

Study population

Normal group (group N) was consisted with 17 healthy volunteers (2 women, 15 men), aged 35±11 years old. They had normal rest electrocardiogram, no history of cardiac event, no coronary risk factors. Mild to moderate disease group (group M) was consisted with 20 patients (5 women, 15 men), aged 59±9 years old. Activities of perfusion defects on PET images were greater than 60% of maximum activity and size of these defects were smaller than 10% of left ventricle. In the group M, 4 patients had one-vessel disease, 4 had two-vessel disease and 12 had three-vessel disease by CAG. Severe disease group (group S) was consisted with 10 male patients, aged 61±9 years old. Activities of perfusion defects on PET images were smaller than 60% of maximum activity and size of these defects were greater than 10% of left ventricle. In the group S, 1 patient had one vessel disease, 3 had two-vessel disease and 6 had three-vessel disease.

Methods

PET imaging

PET imaging of myocardial perfusion at rest and after dipyridamole was carried out as previously described[5-7]. Patients stopped smoking 4 hours before the PET study, fasted for 8 hours, and stopped intake of caffeine and theophylline for 24 hours before the PET study. PET was performed using the University of Texas designed cesium florid, multislice tomograph with a reconstructed resolution of 12mm full-width at half-maximum (FWHM) in plane and 14mm FWHM axially. Transmission images containing 100 to 150 million counts were obtained to correct for photon attenuation with the segmented attenuation method first reported from this laboratory[8]. Emission images were obtained after injection of 15-20 mCi cyclotron-produced N-13 ammonia and contained 20 to 40 million counts (rest scan). At 40 minutes after administration of the first dose of N-13 ammonia, dipyridamole was injected 0.568 mg/kg over 4 minutes or 0.84 mg/kg over 6 minutes. Four minutes handgripping was also performed during dipyridamole injection. Four minutes after the dipyridamole infusion was completed, same dose of N-13 ammonia was injected intravenously and 4 minutes later, PET imaging was repeated by the same protocol used for the resting study (stress scan). Data was acquired for 20 minutes starting at 5 minutes after tracer injection. Aminophylline (125 mg) was given for angina.

Automated quantitative analysis of PET

Automated analysis of PET abnormalities was carried out without observer bias with previously described software[5-7]. A three-dimensional (3D) restructuring algorithm generated short- and long-axis views from PET transaxial cardiac images perpendicular to and parallel to, respectively, the long axis of the left ventricle. To avoid the spatial distortion inherent in polar displays, circumferential profiles were used to reconstruct 3D topographic views of the left ventricle reflecting relative regional activity. The 3D topographic views were divided into fixed

sections consisting of a septal, anterior, lateral and inferior quadrant as previously illustrated[5,7]. A mean algorithm determined, for each of the 3D topographic views, the mean activity level in each of these 4 regions expressed as relative activity levels normalized to the maximum 2% of pixels for the whole-heart data set for each of the 3D topographic views. Finally, an algorithm automatically identified regions of each topographic view that have values deviating outside ±2-SD limits of normal values (4-SD range) on the basis of 17 normal volunteers and computed the percent of circumferential profiles units ±2-SD limits (4-SD range).

Analysis of the relative distribution of activity along the long axis of the ventricle

The 3D restructuring algorithm generated 32 tomographic slices perpendicular to the long axis of the left ventricle labeled slice 1 at the base of the heart to slice 32 at the apex of the heart. Slices 1 through 7 and 30 through 32 were discarded as a result of count variability caused by the membranous septum, by variability in locating the last apical slice, and by partial volume errors resulting from small object size at the apex. For each slice 8 through 29, the average relative activity expressed as percent of maximum was determined for each slice in the septal, anterior, lateral and inferior quadrants. The relative activity of each slice in each quadrant was plotted on the vertical axis for slice 8 through 29 on the horizontal axis for each quadrant of the heart.

The distribution of activity from base (slice 8) to apex (slice 29) was then best fit to a third-degree polynomial as previously described[3]. The relative activity for each slice and slope value for each slice 8 to 29 were then also plotted on the vertical axis for slice number on the horizontal axis for each quadrant.

Rest and dipyridamole images were analyzed similarly for average relative uptake in each quadrant, for longitudinal distribution of relative activity for each quadrant, and for the rate of change in activity or slope along the long axis of the left ventricle. Mean values and ±2-SD limits of relative activity were determined for each slice 8 to 29 for each quadrant for the 17 normal volunteers. The ±2-SD limits of this normal group were plotted for each slice as reference limits on the graphs of relative uptake and slope for each patient. The maximum rate of decrease in relative activity along the long axis of the left ventricle (maximum negative slope or minimum slope value including the sign) was determined for each quadrant of each patient.

Statistical analysis

Data are reported as mean ± SD. The significance of differences between groups was determined by two-tailed non-paired Student's *t-test* and P values <0.05 were considered significant.

Ⅲ. Results

Figure 1 demonstrated the PET images in each group. Average relative activity in each group in each quadrant was compared for each tomographic slice from base to apex (Fig. 2-5).

Comparison between the group M and the group N

Average relative activities of the group M in anterior, lateral and inferior quadrants progressively and significantly decreased from base to apex slices compared to the group N ($P<0.05$). The septal quadrant showed a similar trend that did not reach statistical

significance, as expected due to effects of the membranous septum and fluid dynamic, branching pattern.

Comparison between the group S and the group N

In all quadrants, average relative activities of the group S progressively and significantly decreased from base to apex slices compared to the group N ($P<0.05$). If two patients with severe local basal inferior perfusion defects were included, average relative activity was significantly low from basal to apical slices (Fig. 5A). Without these two cases, average relative activity was significantly low from middle to apex slices and the longitudinal base to apex gradient was steeper (Fig. 5B).

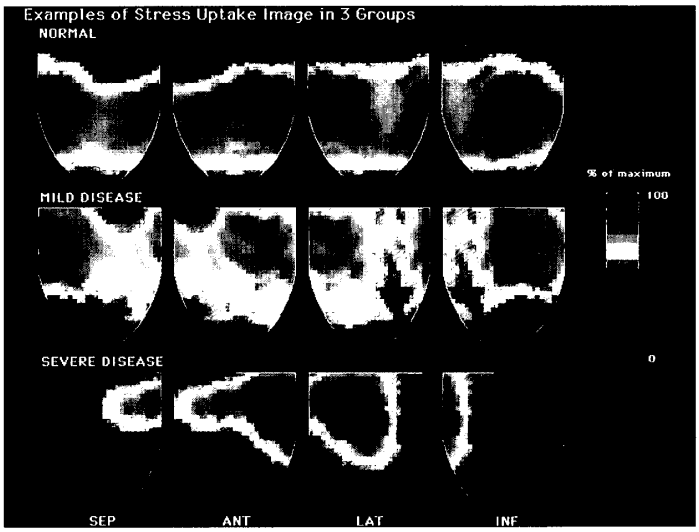

Fig. 1
^{13}N-ammonia PET image after dipyridamole administration in group N, group M and group S in each quadrant.

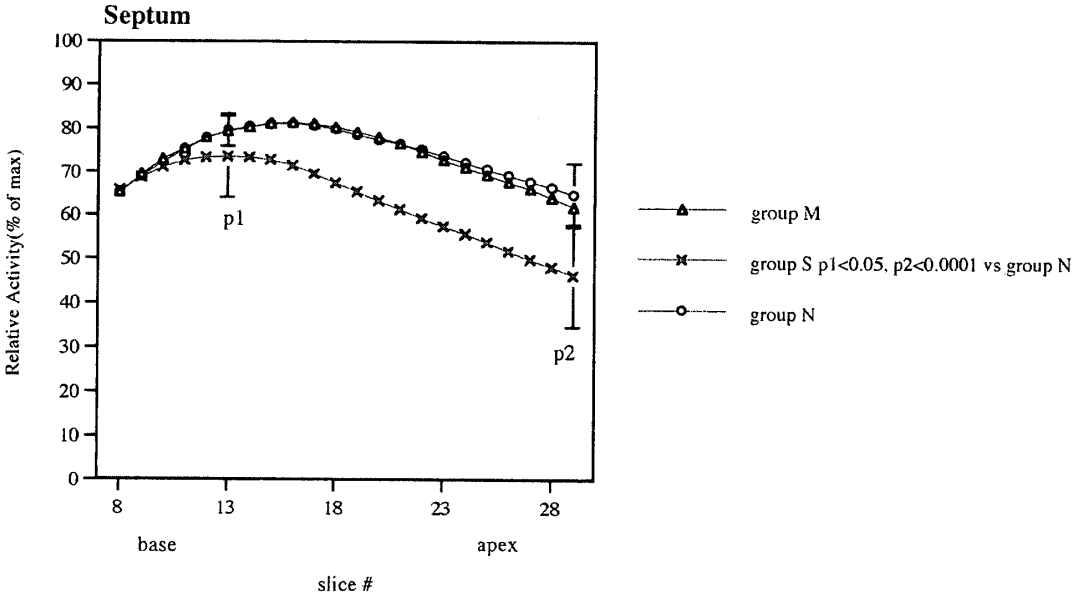

Fig. 2
Average relative activities in septal quadrant. In group M, average relative activities decreased from base to apex compared to group N, but did not reach statistical significance. In group S, average relative activities progressively and significantly decreased from base to apex slices compared to the group N ($P<0.05$).

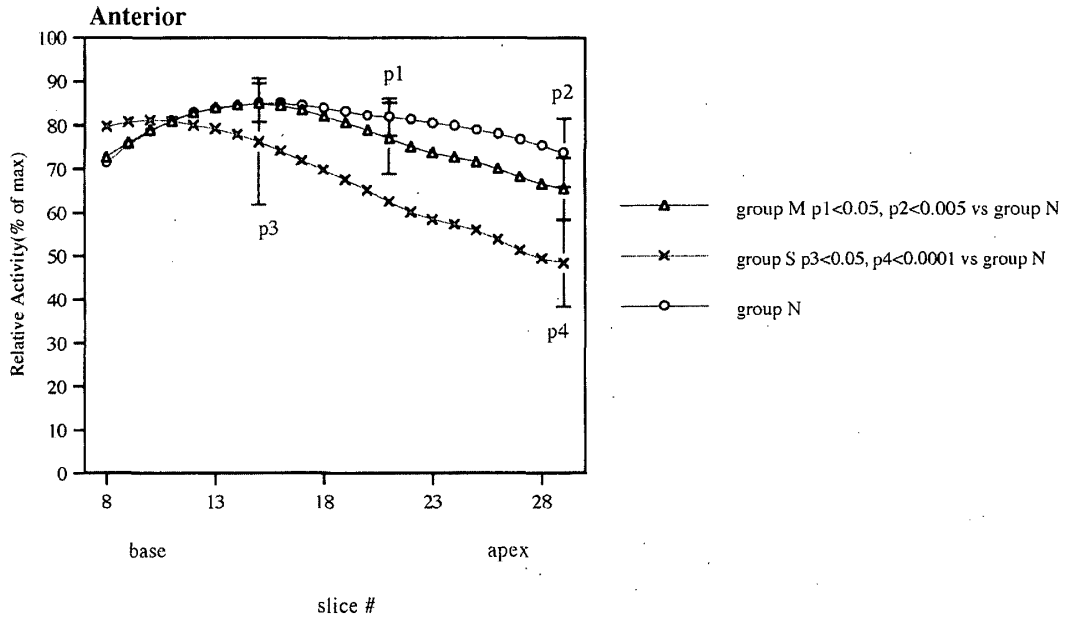

Fig. 3
Average relative activity in anterior quadrant in each group. In both group M and S, average relative activities progressively and significantly decreased from base to apex slices compared to the group N ($P< 0.05$).

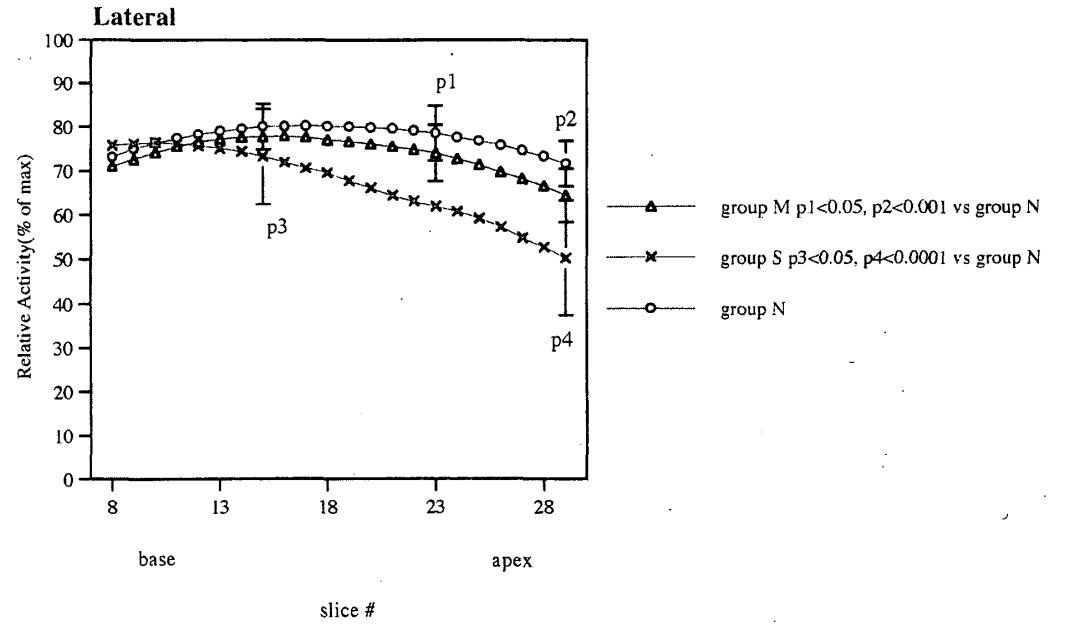

Fig. 4
Average relative activity in lateral quadrant in each group. In both group M and S, average relative activities progressively and significantly decreased from base to apex slices compared to the group N ($P< 0.05$).

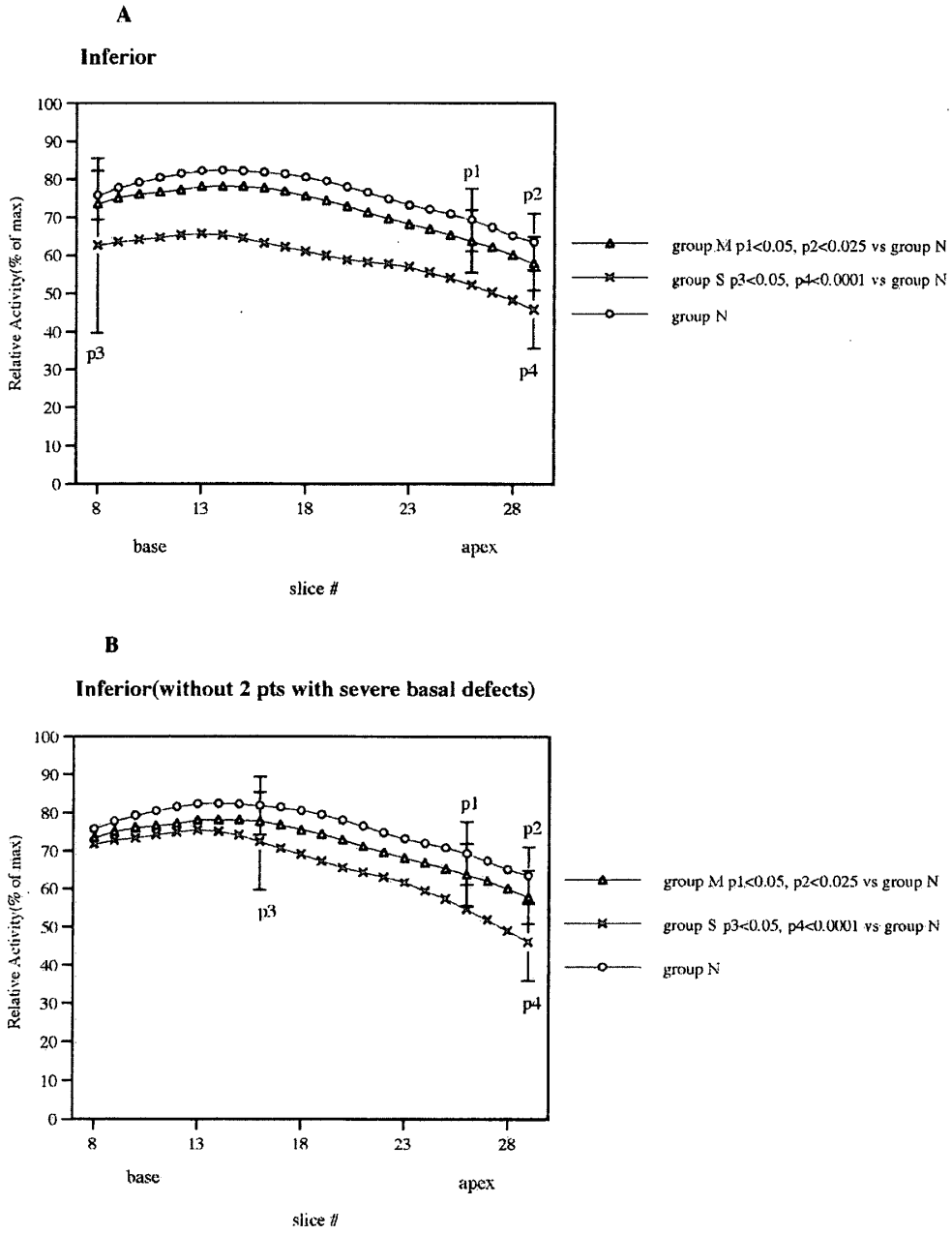

Fig. 5
Average relative activity in inferior quadrant in each group. Fig. 5A showed average relative activity in each group in inferior quadrant including two cases with local basal perfusion defect. Without these two cases, the tendency of the longitudinal base to apex perfusion gradient was the same as the other quadrants.

Table 1 shows the relation between CAG findings and average relative activity in each quadrant in each patient group which was below 2 standard deviations of the normal mean expressed as % of slices. Ten out of 12 patients with only one-vessel disease or two-vessel disease of 20% diameter stenosis or greater had abnormal relative activity and base to apex longitudinal perfusion gradients without corresponding arteriographic stenosis of the artery to abnormal PET regions.

Table 1
The relation between CAG findings and average relative activity in each quadrant in each patient group which was below 2 standard deviations of the normal mean expressed as % of slices.

Group M (n=20)					% of slices<-2s.d.							
patient No.	CAD	RCA	LAD	LCX	sep(R)	ant(R)	lat(R)	inf(R)	sep(S)	ant(S)	lat(S)	inf(S)
1	3	+	+	+	0	0	27	32	14	0	41	73
2	3	+	+	+	0	0	0	0	0	0	0	0
3	3	+	+	+	0	0	0	0	0	0	0	0
4	2	+	+		5	0	18	0	23	5	0	0
5	3	+	+	+	47	35	26	26	12	12	0	0
6	1		+		0	0	9	0	0	0	0	0
7	1		+		0	0	0	0	0	0	0	0
8	2	+	+		0	36	45	0	0	9	0	0
9	2		+	+	27	5	5	0	0	0	0	0
10	3	+	+	+	0	5	0	0	0	0	0	0
11	3	+	+	+	0	0	0	0	0	0	0	14
12	1		+		23	50	9	0	95	86	9	0
13	3	+	+	+	45	68	9	0	50	73	82	14
14	3	+	+	+	68	59	0	0	41	59	36	0
15	3	+	+	+	5	0	23	0	0	0	23	0
16	1	+			41	18	0	0	45	0	0	0
17	3	+	+	+	0	0	0	0	0	0	0	50
18	3	+	+	+	0	14	9	0	0	50	45	0
19	3	+	+	+	0	0	0	0	0	11	9	0
20	2		+	+	0	0	0	36	0	0	0	64

Group S (n=10)					% of slices<-2s.d.							
patient No.	CAD	RCA	LAD	LCX	sep(R)	ant(R)	lat(R)	inf(R)	sep(S)	ant(S)	lat(S)	inf(S)
1	3	+	+	+	0	0	5	0	86	77	41	100
2	2		+	+	18	68	0	0	82	91	73	5
3	3	+	+	+	0	5	41	82	73	50	86	100
4	3	+	+	+	0	23	18	68	0	91	86	100
5	3	+	+	+	0	0	0	0	50	0	0	9
6	2	+	+		27	68	50	27	50	68	23	23
7	1		+		36	0	9	14	27	32	5	0
8	2	+	+		45	0	0	68	59	45	55	86
9	3	+	+	+	86	0	18	0	95	68	14	0
10	3	+	+	+	0	0	59	0	0	9	91	0

□ : no stenotic artery on CAG, abnormal PET

IV. Discussion

Coronary arteriography has been considered as a diagnostic "gold standard" for determining coronary stenosis; however, this invasive method often failed to detect diffuse coronary atherosclerosis. Gould et al. first demonstrated the longitudinal base-to-apex myocardial perfusion abnormalities by PET non-invasively in our previous study[3]. In the present study I indicated that both group M and S had abnormal longitudinal perfusion gradient compared with group N, and especially group S showed longitudinal gradient even in the middle of the heart. Donohue et al. reported that abnormal perfusion imaging patients indicated higher proximal / distal coronary flow velocity reserve ratio(CFVR) and this result supports my data[9].

Endothelial dysfunction plays an important role for coronary atherosclerosis. I used dipyridamole for coronary vasodilation in the

present study. Dipyridamole is known as an endothelial-independent vasodilator, and dipyridamole-induced coronary vasodilation is a result of an adenosine effect on resistance vessels mediated by inhibition of the reuptake of adenosine released by cardiac myocytes. Also, hyperemia induced by vasodilation of resistance vessels causes secondary coronary vasodilation and which is endothelial-dependent. In my cases, diseased groups showed longitudinal base-to-apex perfusion gradients, especially in severe diseased group. I could suppose that coronary atherosclerosis impaired more extensive and that affected the vasodilation induced by dipyridamole. On the other hand, Masoli et al. showed the data which evaluated the relation between invasive angiographic measurements of coronary vasomotion in response to intracoronary acetylcholine and the presence of regional perfusion abnormalities assessed by Tc-99m sestamibi myocardial perfusion imaging[10]. They indicated that 4 out of 13 angiographically normal coronary arteries had a vasoconstrictive response to acetylcholine, which was associated with a regional perfusion defect. Acetylcholine is known as an endothelial-dependent vasodilator and it causes vasodilation in normal coronary arteries, whereas it elicits paradoxical vasoconstriction in diseased vessels. Despite the differences of vasodilator, the data from Masoli et al. supported my results and I could suspect that endothelial dysfunction caused perfusion abnormalities.

Also, some of the patients with one or two-vessel disease showed perfusion abnormalities in the "stenosis-free" regions by CAG. I could suppose that patients with segmental coronary artery disease had diffuse coronary atherosclerosis even in stenosis-free coronary artery by arteriography, which could be detected by PET non-invasively.

In conclusion, patients with segmental coronary artery disease by arteriography have abnormal longitudinal base to apex perfusion gradients on dipyridamole PET images indicating diffuse coronary atherosclerosis. Longitudinal analysis of PET perfusion images show a characteristic perfusion pattern of diffuse coronary artery narrowing which is not revealed by segmental stenosis on coronary arteriograms.

Acknowledgements

The author thanks Dr. Keiichi Nakagawa and Dr. Katsuya Yoshida for their assistance in performing PET studies; Dr. K. Lance Gould and Dr. Yoshiaki Masuda for their coordination of the project.

要　旨

瀰漫性冠動脈硬化は通常限局性狭窄に伴うと考えられるが，現行の非侵襲的検査や冠動脈造影では捉え難い。そこで正常群（17名）と冠動脈造影で狭窄を有する患者群（30名）にジピリダモール負荷N-13アンモニアポジトロンCTを行い心基部から心尖部への長軸的血流分布を評価した。心血流像を心長軸沿に25短軸像にわけ，各短軸像を前壁，左室中隔，左室側壁，後壁にわけた。各側面で各短軸像の相対血流値を長軸方向にグラフ表示し3次式近似を行った。中等度血流欠損群（20名）は左室中隔以外で心尖部で血流低下を認め，高度血流欠損群（10名）は，全側面で左室中央部から高度な血流低下を認めた。一枝及び二枝疾患患者12名は，冠動脈造影上狭窄を認めない領域で血流欠損像を認めた。限局性冠動脈病変を有する患者で，ジピリダモール負荷ポジトロンCTで心臓長軸方向で血流分布の低下を認め，瀰漫性冠動脈硬化が示唆された。冠動脈造影で認め難い瀰漫性冠動脈硬化を，ポジトロンCTの血流分布で捉えられると思われた。

References

1) Falk E, Shah PK, Fuster V. Coronary plaque disruption. Circulation 1995; 92: 657-71.
2) Farb A, Tang AL, Burke AP, Sessums L, Liang Y, Virmani R. Sudden coronary death: frequency of active coronary lesions, inactive coroanry lesions, and myocardial infarcrion. Circulation 1995; 92: 1701-9.
3) Gould KL, Nakagawa Y, Nakagawa K, Sdringola S, Hess MJ, Haynie M, Parker N, Mullani N, Kirkeeide R. Frequency and clinical implications of fluid dynamically

significant diffuse coronary artery disease manifest as graded, longitudinal, base-to-apex myocardial perfusion abnormalities by noninvasive positron emission tomography. Circulation 2000 ; 101 : 1931-9.
4) Mintz GS, Painter JA, Pichard AD, Kent KM, Salter LF, Popma JJ, Chuang YC, Bucher TA, Sokolowicz LE, Leon MB. Atherosclerosis in angiographically "normal" coroanry artery reference segments: an intravascular ultrasound study with clinical correlations. J Am Coll Cardiol 1995 ; 25 : 1479-85.
5) Gould KL. Coronary artery stenosis and reversing atherosclerosis. 2nd ed. Arnold Publishing : New York: Oxford University Press ; 1999.
6) Demer LL, Gould KL, Goldstein RA, Kirkeeide RL. Diagnosis of coronary artery disease by positron emission tomography: comparison to quantitative coronary arteriography in 193 patients. Circulation 1989 ; 79 : 825-35.
7) Gould KL, Martucci JP, Goldberg DI, Hess MJ, Edens RP, Latifi R, Dudrick SJ. Short-term cholesterol lowering decreases in size and severity of perfusion abnormalities by positron emission tomography after dipyridamole in patients with coronary artery disease. Circulation 1994 ; 89 : 1530-8.
8) Xu EZ, Mullani NA, Gould KL, Anderson WL. A segmented attenuation correction for PET. J Nucl Med 1991 ; 32 : 161-5.
9) Donohue TJ, Miller DD, Bach RG, Tron C, Wolford T, Caracciolo EA, Aguirre FV, Younis LT, Chaitman BR, Kern MJ. Correlation of poststenotic hyperemic coronary flow velocity and pressure with abnormal stress myocardial perfusion imaging in coronary artery disease. Am J Cardiol 1996 ; 77 : 948-54.
10) Masoli O, Balino NS, Sabate D, Jalon J, Meretta A, Cragnolino D, Sarmiento R, DiCarli MF. Effect of endothelial dysfunction on regional perfusion in myocardial territories supplied by normal and diseased vessels in patients with coronary artery disease. J Nucl Cardiol 2000 ; 7 : 199-204.